Available online at www.sciencedirect.com

jmr&t Journal of Materials Research and Technology

www.jmrt.com.br

Original Article

Different time's Nd:YAG laser-irradiated PVA/Ag nanocomposites: structural, optical, and electrical characterization

Islam Shukri Elashmawi[a,b], *Abdelrhman Anter Menazea*[b,c,*]

[a] *Physics Department, Faculty of Science at Al-Ula, Taibah University, Madina, Saudi Arabia*
[b] *Spectroscopy Department, Physics Division, National Research Centre, Dokki, 12311 Giza, Egypt*
[c] *Laser Technology Unit, National Research Centre, Dokki, 12311 Giza, Egypt*

ARTICLE INFO

Article history:
Received 30 November 2018
Accepted 24 January 2019
Available online 12 March 2019

Keywords:
PVA
Silver
Nd:YAG
XRD
FT-IR
UV–Vis
AC conductivity

ABSTRACT

Composite films of polyvinyl alcohol (PVA)/Silver nanoparticles (AgNPs) were synthesized via casting method. The presence of AgNPs in PVA was approved by an apparition of Surface Plasmon Resonance (SPR) around 427 nm of the composite absorption spectra. The nanocomposite films were irradiated at different times (5, 10, and 15 min) pulsed Nd:YAG laser. The integral intensity of diffracted X-ray photons from films has been increased noticeably after the doping process denotes increasing in the ordering character of the PVA/Ag nanocomposite irradiated to different time's laser, which can be assigned to the reduction that has been induced by laser. Observations of IR spectra indicated that laser enhances the structural modifications between the chains in PVA and the silver nanoparticles with further increasing laser irradiation time. The observed increase in refractive index (n) and the decreasing in the optical band gap of PVA/Ag nanocomposite films after irradiated to the laser with different times (5, 10, and 15 min) comparing with pure PVA suggesting its possibility to using optical device applications. The behavior of ε' and ε'' are gradually decreased with the increase of the frequency. The value of ε' and ε'' are decreases due to the contribution of interfacial polarization effect in dielectric permittivity. The relation between M' and M″ depicts the formation of a semicircle arc indicating the presence of broad relaxation processes.

* *Corresponding author.*
E-mail: aanter7@gmail.com (A.A. Menazea).

https://doi.org/10.1016/j.jmrt.2019.01.011

1. Introduction

In recent years, nanotechnology is a particularly different field, ranging from novel expansions of usual device physics to exactly new approaches to developing new materials have dimensions on the scale of nanometer [1].

Metal nanoparticles have fantastic electronic, optical, and magnetic properties of nanostructures, especially, nanowires and nanorods have been used in the fabrication of new nanodevices and nanocomposites [2,3]. In the last ten years, a great evolution has been carried out on the synthesis and fabrication of one dimensional nanomaterial. Metal nanoparticles integrated polymers attracted great observance because of the widened application goal offered by these hybrid materials [4–6]. Silver nanoparticles have received significant attention due to their interesting physical and chemical properties [7]. It is found in several applications, such as non-linear optics, electronics, catalysis, biomaterial and antimicrobial applications [8].

Polymers have drawn enormous interest in device manufacturing due to their amazing intrinsic properties such as easy processability, flexibility and high mechanical strength. Polymers are also described by stability after physical and chemical doping [9,10].

Many studies have been discussed in literature showed efforts for preparation of the nanoparticles doped polymers, with the possibility of wide in their optical and morphological structure of their application with high performance optoelectronic, electrical, and optical devices, biomedical science, sensors [11,12]. Particularly, polymer/metal nanocomposites such as polymer/Silver nanoparticles composites is promising effective materials in different fields [13,14].

The using of PVA as a good host polymer for silver nanoparticles is favorable because of its excellent thermo-stability, water solubility and chemical resistance [15]. On other words, PVA has gained attention because of its non-toxic, non-carcinogenic, biodegradable, biocompatible qualities, its reduction ability of the secondary alcohol groups and wonderful film-forming properties and optical transparency [16,17].

A number of experimental works with pulsed Nd:YAG laser irradiation has a broad applications concern metal/polymer nanostructures due to its nonlinear response characteristics. The modification in physical properties of metal/polymer nanocomposites can be investigated by irradiated Nd:YAG laser [18]. These modifications are attributing to the amelioration dispersion of nanoparticles in the metal/polymer nanocomposites matrix that resulting from the formation of cross-linking chains.

In this paper, we aim to investigate the laser irradiation time role in modifying the structural, optical, and electrical properties of PVA/Ag nanocomposite. The samples of polyvinyl alcohol/silver (PVA/Ag) nanocomposite films were prepared by adding Ag nanoparticles with 5 wt% to PVA solution. The films of 0.1 mm thickness were prepared by the casting method. The obtained PVA/Ag nanocomposite films have been irradiated to different times of pulsed nanosecond laser. The effect of time of nanosecond laser irradiation on the physical characterizations of PVA/Ag nanocomposites has been investigated using XRD, UV–visible, FTIR and Ac Conductivity. The response transmittance, reflection, optical bandgap, dielectric constant, optical conductivity, dispersion refractive index, and dielectric relaxation time behavior of PVA/Ag nanocomposites films with varying laser irradiation time are also investigated.

2. Materials and method

2.1. Materials

PVA/Ag nanocomposite films were prepared by using; PVA (Mw ≈ 130,000) and Silver nitrate ($AgNO_3$). All the chemicals were purchased from Sigma Aldrich used without further purification. Double distilled water (DDW) was used as a solvent.

2.2. Synthesis pure PVA and PVA/Ag nanocomposite films

Pure PVA and PVA/Ag nanocomposites were synthesized by chemical reduction method. PVA solution was prepared by dissolving PVA powder 5 wt% of PVA powder (5 g in 100 ml DDW) with continuous stirring at 65 °C for 4 h. Pure PVA solution cooled down to room temperature. Freshly prepared cold $AgNO_3$ aqueous solution with concentration (0.03 wt%) was added dropwise to PVA solution in a darkroom with continuous stirring for 2 h. The color of the solution was changed from colorless to light yellowish; AgNPs were obtained by the following heating the solution. The final solution of PVA/$AgNO_3$ was poured into Petri then kept drying to get films via casting at the room temperature in a dark room for 4 days.

2.3. Laser irradiation process to PVA/Ag nanocomposite films

The prepared sample with 0.1 mm thickness was irradiated via fundamental wavelength ($\lambda = 1064$ nm) nanosecond (Nd:YAG) laser (Continuum laser, Elctro-optics, Inc. Model: PRII 8000 with 3.8 W power, 10 Hz repetition rate, and 8 ns pulse duration. The prepared samples were irradiated to a different time; 5, 10, and 15 min. The laser beam was incident to the surface of the PVA/Ag nanocomposite films using quartz concave lens with 100 mm focal length. The incident laser spot diameter has been measured as 4.5 mm. The target film was far 20 cm from the laser source, approximately.

2.4. Characterization

The X-ray diffraction patterns were obtained via PANalytical X'Pert Pro XRD system occupied with Cu-Kα radiation ($\lambda = 0.154$ nm), and work at 45 kV, the scans were collected over a 2θ range from 5° to 80°. The optical measurements [Absorption (A) and Transmission (T)] as a function of wavelength λ (nm) of the prepared samples were measured using JASCO (V-570) UV/VIS/NIR double beam spectrophotometer at room temperature in the wavelength region of 200–1000 nm. FTIR spectral data were collected through 32 scans with resolution 2 cm^{-1} using Nicolet is 10 single beam spectrometer via KBr powder route in mid IR spectral wavenumber range

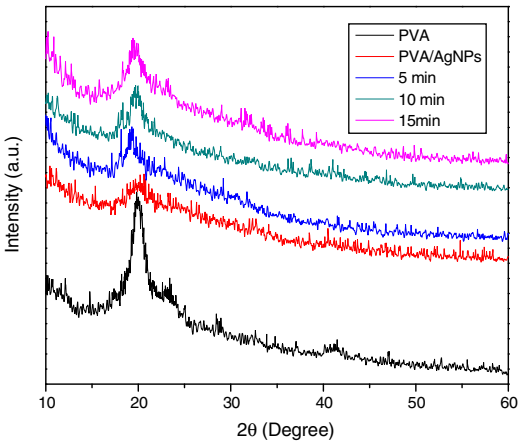

Fig. 1 – XRD patterns for pure PVA and PVA/Ag nanocomposite films before and after irradiated to different times of nanosecond laser (5, 10, 15 min).

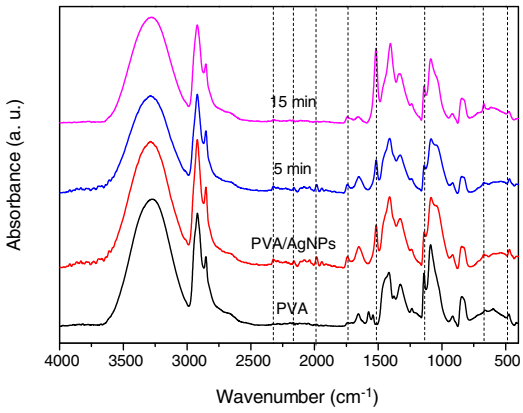

Fig. 2 – FT-IR absorption spectra for pure PVA and PVA/Ag nanocomposite films before and after irradiated to different times of nanosecond laser (5, 10, and 15 min).

4000–400 cm^{-1} to examine their structure. AC conductivity measurements were carried out by using The Broadband Dielectric Spectroscopy (BDS) type (concept 40) Novocontrol High Resolution Alpha Analyzer assisted by Quatro Temperature Controllers using pure nitrogen as the heating agent. The samples were measured at 30 °C using frequency from 0.1 Hz to 7 MHz.

3. Results and discussion

3.1. *X-ray diffraction*

To study the effect of different time's laser irradiation on the structure and degree of ordering of PVA/Ag nanocomposites, XRD measurements were carried out on the thick films over the 2θ angular range 10–60°, at room temperature.

Fig. 1 obtains XRD patterns for pure PVA, PVA/Ag nanocomposite and PVA/Ag nanocomposites irradiated to a laser with different times. XRD of Pure PVA indicates a two characteristic diffraction bands at (2 theta) = 20 and 41 degrees assigned as [101], [200] that attributed to the semi-crystallinity of PVA polymer [19], that might be related to the strong intramolecular and intermolecular hydrogen bonding between PVA molecular chains. The intensity of the beak at 2 theta = 20 deceased in PVA/Ag nanocomposites because of the complexation of AgNPs in PVA before irradiation. It was obtained that XRD pattern of the samples at different time of laser radiation is characterized by halos extending in the 2 theta range from 17 to 22, with maximum intensity at 20 [20].

The integral intensity of diffracted X-ray photons from films has been increased noticeably after the doping process indicates that there was an increase in the character ordering in PVA/Ag nanocomposites irradiated to different time's laser, which can be assigned to degradation resulted by laser [21].

3.2. *FTIR analysis*

FTIR is an important technique used for investigation structure changes in PVA/Ag nanocomposite due to laser irradiation, where it illustrates interactions between the various consistent related to the induced changes in the band position and the vibration modes. The absorption spectra of infrared for PVA, PVA/Ag nanocomposites, PVA/Ag nanocomposites films that irradiated to nanosecond laser with times (5 and 15 min) are sown in Fig. 2. The distinctive absorption peak of pure PVA was obtained at 3580 cm^{-1}, 2974 cm^{-1}, 1741 cm^{-1}, 1570 cm^{-1}, 1460 cm^{-1}, 845 cm^{-1} [22,23]. Pure PVA curve showed a broad and strong absorption band between 3400 cm^{-1} and 3200 cm^{-1} that attributed to vibration stretching in the O-H group that approved the existence of hydroxyl group. The band that obtained at 2922 cm^{-1} was due to the anti-symmetric CH_2 stretching vibration. The absorption bands at 1741 cm^{-1} and 1570 cm^{-1} were a result stretching vibration in C=O. The band at 1460 cm^{-1} is attributed to vibrations bending in C–H and O–H. The absorption bands at 1400 and 1300 cm^{-1} were related to wagging vibrations in C–H and CH_2, respectively. The presence of band at 1140 cm^{-1} was attributed to stretching vibrations in C–O–C and C–O while the band that obtained at 910 cm^{-1} and 838 cm^{-1} were attributed to stretching vibration in C–C and out of plane bending in O–H, respectively [24].

The broadening and the little decreasing in the intensity that obtained in the absorption bands range from 3400 cm^{-1} to 3200 cm^{-1}, 2974 cm^{-1}, 1741 cm^{-1}, 1468 cm^{-1} and vanishing of bands at 1560 cm^{-1}, 1631 cm^{-1}, and 1384 cm^{-1} obviously propose the interaction that occurred between AgNPs and PVA in the PVA/Ag nanocomposite.

At different laser irradiation times, it was observed that the intensity bands at 3400 cm^{-1}, 3200 cm^{-1}, 1741 cm^{-1}, 1460 cm^{-1}, 1300 cm^{-1}, 1147 cm^{-1}, and 910 cm^{-1} was decreased and shifted as times of laser irradiation increasing. Decreasing the intensity of peaks in FTIR spectrum confirms that after doping, numbers of PVA chains are increased in the structure of the films. The previous observations illustrate the structure rearrangement between PVA and AgNPs that caused by further times of laser irradiation.

3.3. *Optical spectroscopy*

Fig. 3 shows the absorption spectra of pure PVA, PVA/Ag films, PVA/Ag nanocomposite samples irradiated by different times

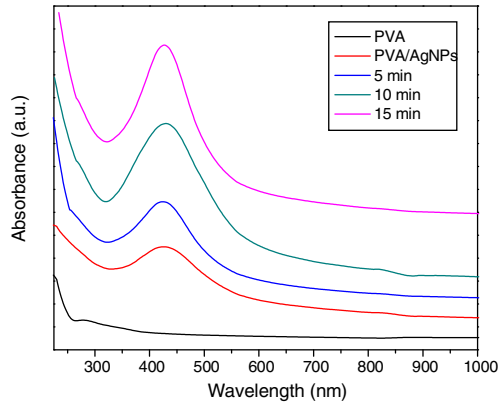

Fig. 3 – UV–visible absorbance spectra for pure PVA and PVA/Ag nanocomposite films before and after irradiated to different times of nanosecond laser (5, 10, and 15 min).

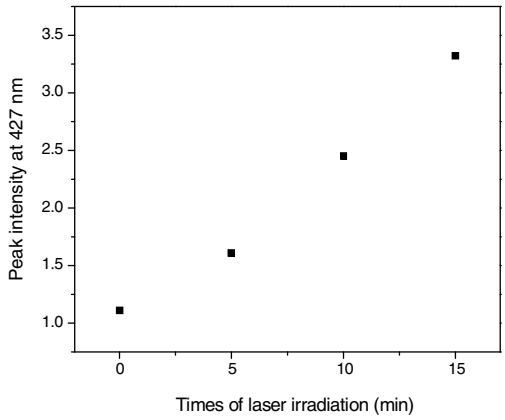

Fig. 4 – The relation between the different times of laser irradiation and the peak intensity at 427 nm.

of nanosecond laser. Fig. 3 obviously showed no absorption peak for PVA within the UV range excepting the little absorption peak that appeared at 276 nm, that mainly attributed to transition between the PVA and AgNPs ($n\rightarrow\pi^*$) resulting from the carbonyl group (C=O) [25]. The UV–Vis absorption spectra obtain an evident characteristic absorption peak at 427 nm attributed to the SPR effect, supporting the existence of AgNPs in PVA. Fig. 3 showed that the peak at 427 nm was increased as the irradiation time of nanosecond laser increased. This attitude was observed clearly in Fig. 4, that obtain the relation between the different times of laser irradiation and the peak at 427 nm that due to the laser power was enough to make a full reduction of silver nitrate to AgNPs and increasing in the silver inside the PVA/Ag nanocomposites [26]. Due to the laser irradiation increases the reaction between AgNPs and PVA which clarified obviously in the absorption spectra increasing.

The optical absorption coefficients α of the prepared samples as a function of the wavelength λ can be directly calculated using this equation [27]:

$$\alpha(\lambda) = \frac{2.303}{d} A \quad (1)$$

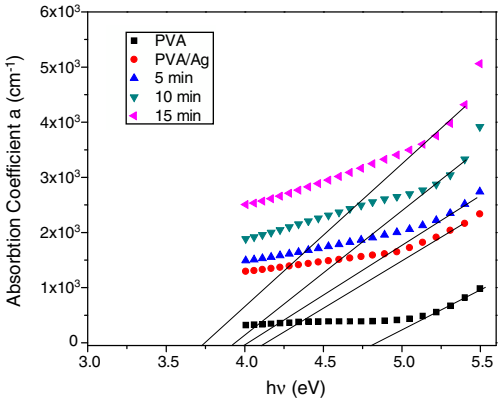

Fig. 5 – Relation between absorption coefficient (α) versus ($h\upsilon$) for pure PVA and PVA/Ag nanocomposite films before and after irradiated to different times of nanosecond laser (5, 10, and 15 min).

where A is the absorbance and d is the thickness of the sample. Fig. 5 reveals the optical absorption coefficient relative to photon energy for pure PVA, PVA/Ag nanocomposites, PVA/Ag nanocomposites films irradiated to nanosecond laser at different times.

It was obtained that the increases of laser irradiation time make a clear shift toward smaller photon energies in absorption edge. Also, it was obtained that α increased with increasing photon energy $h\upsilon$ and laser irradiation time. The values of absorption edge are recorded in Table 1; it can see that the absorption edge is 4.81 eV for pure PVA and 4.12 eV for PVA/Ag nanocomposites. The absorption edge has drastically decreased one by one by increasing the laser irradiation times from 5 min to 15 min until reached the value of 3.72 eV.

The optical band gap E_g for the unirradiated and irradiated films to different times of laser can be calculated by using the Tauc's relation [28]:

$$\alpha h\upsilon = A(h\upsilon - E_g)^m \quad (2)$$

where$h\upsilon$ is the photon energy, A is the band tailing parameter and $m = 1/2$ for direct energy gap, and $m = 2$ for indirect energy gap.

The direct and indirect energy band gap for pure PVA, PVA/Ag nanocomposites and PVA/Ag nanocomposites irradiated to nanosecond laser at different times, $(\alpha h\upsilon)^{1/2}$and $(\alpha h\upsilon)^2$ were obtained as a function of $h\upsilon$ in Figs. 6 and 7, respectively. According to the intercept of the best fit of lines in x-axis, the values of direct and indirect energy band gaps had been calculated from these figures and recorded in Table 1.From Figs. 6 and 7 and Table 1, it was observed that the values of direct and indirect energy band gap for pure PVA were 4.42 eV and 3.96 eV, respectively, and for unirradiated PVA/Ag nanocomposites the values were 4.31 eV and 3.33 eV, respectively. This value of PVA/Ag nanocomposites can be assigned to the chemical bond that formed between PVA and AgNPs that lead to the generation of localized states between High Occupied Molecular Orbital (HOMO) and Lower Unoccupied Molecular Orbital (LUMO) energy bands making the lower energy transitions feasible [29]. Observable decreasing in the

Table 1 – Values of absorption edge, direct, indirect optical energy gap and refractive index of PVA/Ag nanocomposite films before and after irradiated to different times of nanosecond laser (5, 10, and 15 min).

Samples		Absorption edge (eV)	Direct energy gap (eV)	Indirect energy gap (eV)	Refractive index (*n*)
Before laser	PVA	4.81	4.42	3.96	2.18
	PVA/AgNPs	4.12	4.31	3.33	2.31
After laser	5 min	4.00	4.21	3.01	2.39
	10 min	3.92	3.95	2.19	2.66
	15 min	3.73	3.79	1.94	2.77

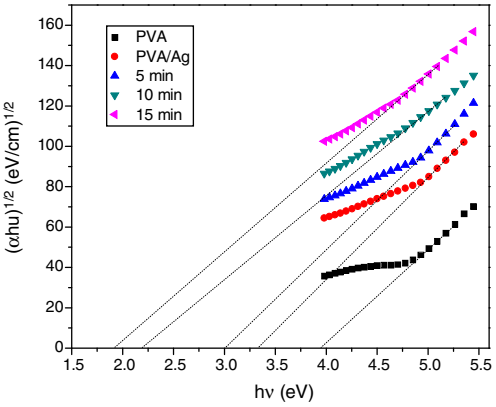

Fig. 6 – Plots of $(\alpha h\nu)^{1/2}$ versus photon energy ($h\nu$) for pure PVA and PVA/Ag nanocomposite films before and after irradiated to different times of nanosecond laser (5, 10, 15 min).

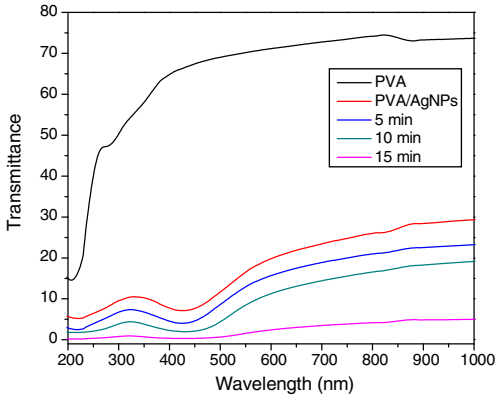

Fig. 8 – UV–visible transmittance spectra for pure PVA and PVA/Ag nanocomposite films before and after irradiated to different times of nanosecond laser (5, 10, and 15 min).

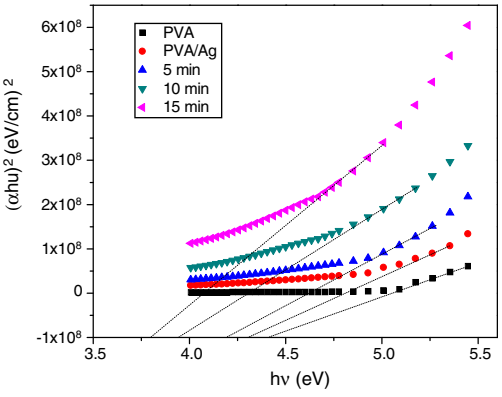

Fig. 7 – Plots of $(\alpha h\nu)^2$ versus photon energy ($h\nu$) for pure PVA and PVA/Ag nanocomposite films before and after irradiated to different times of nanosecond laser (5, 10, 15 min).

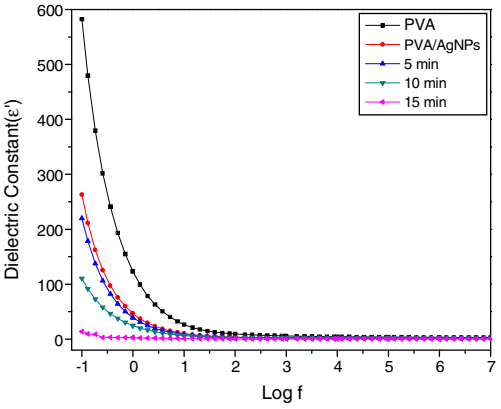

Fig. 9 – Typical plots of variation of real part of the dielectric constant (ε') with frequency for pure PVA and PVA/Ag nanocomposite films before and after irradiated to different times of nanosecond laser (5, 10, 15 min) at room temperature.

values of direct and indirect energy band gap for PVA/Ag nanocomposite irradiated to different times of laser irradiation has been shown with increasing the laser irradiation time from 5 min to 15 min and approaches 3.79 eV, 1.94 eV, respectively at the time of 15 min. This discussion indicating that, as the laser irradiation time increases, the number of silver ions increased in PVA matrix making an increase in the conjugation between AgNPs and the unsaturated bonds of PVA purposed the reduction in the energy band gap .

The variation transmittance (T) for pure PVA, PVA/Ag nanocomposites, and PVA/Ag nanocomposites films irradiated to nanosecond laser at different times as a function of wavelength as shown in Fig. 8. The transmission of PVA was approximately in the visible region from 400 to 800 nm with a teeny reduction at lower wavelengths in the range of 215 to 255 nm is due to the existence of the PVA polymer bandgap confirming almost its transparent nature [30].

For unirradiated PVA/Ag nanocomposites, the transmission reduces significantly and a hollow at 445 nm has been

created, this new valley is assigned to the formation of charge transfer complexes [31]. The presence of this valley in the visible region is attributed to SPR nature of the AgNPs embedded in PVA. The visible screening of the pure PVA and PVA/Ag nanocomposites films indicates the observable color changes in the films. Further, it is clear from the figure that after laser irradiation, the transmission decreased drastically at 215 nm, 325 nm, and 445 nm by increasing the time of laser irradiation from 5 in to 15 min, resulting, the light yellowish color of PVA/Ag nanocomposites films was changed to pale yellow and then brown yellowish after laser irradiation with increasing time. It was clearly indicating that at 15 min time, the transmission is as very good as vanish to zero in UV region, offering these PVA/Ag nanocomposites films after irradiation can utilizing for shielding purposes from UV photons.

The refractive index n was calculated in terms of indirect energy band gap according to Dimitrov and Sakka relation [32]:

$$\frac{n^2-1}{n^2+2} = 1 - \sqrt{\frac{E_g}{20}} \tag{3}$$

The values of n that are tabulated in Table 1 show increasing trend byan increasing in the time of laser irradiation. The increasing in the laser irradiation time from 5 min to 15 min led to increase the scattering of the incident light and as well the speed of light passing through is decreased according to the relation ($n = c/v$) where, c is the velocity of light in free space and v is the velocity of light in the material, thereby the refractive index was increased.

The observed increase in refractive index (n) and also, the decreasing in the optical energy band gap of PVA/Ag nanocomposites films before and after irradiated to laser with different times in comparison with pure PVA proposing it's a possibility to using an optical device application.

3.4. AC electrical conductivity

3.4.1. The dielectric analysis

Fig. 9 displays the plot of the dielectric constant (ε') as a function of frequency Log (f). Fig. 10 shows the plot between the dielectric loss (ε') and the frequency Log (f) for pure PVA and PVA/Ag nanocomposites irradiated to nanosecond laser at different times. The plots of both ε' and ε'' (as shown in the two figures) are gradually decrease with the increase of the frequency and it reaches to constant values at higher frequency. This behavior is due to high contribution of charge accumulation at the samples. Generally, the values of ε' and ε'' are high at low frequency and decreasing with the increase of frequencies ascribed to polarization effects [33,34]. Moreover, there are three regions shown in the behavior of ε' and ε'' over the range of frequency range [35]. At low frequencies, the values of ε' and ε'' are decreases due to the contribution of interfacial polarization effect in dielectric permittivity. At intermediate frequency, the dielectric dispersion is attributed to the dipolar polarization of polymers chain segments. The non-linearity behavior of ε' and ε'' is decreased with the increase of frequency.

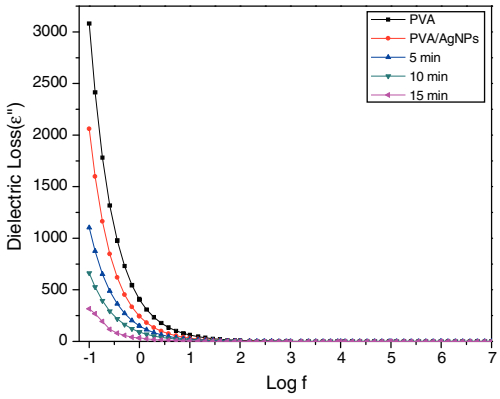

Fig. 10 – Typical plots of variation of imaginary part of the dielectric constant (ε'') with frequency for pure PVA and PVA/Ag nanocomposite films before and after irradiated to different times of nanosecond laser (5, 10, 15 min) at room temperature.

3.4.2. Complex modulus

The mathematical equation complex modulus (M*) can be evaluated as [36]:

$$M^* = M' - jM'' = \frac{1}{\varepsilon^*} = \frac{\varepsilon' + j\varepsilon''}{(\varepsilon')^2 + (\varepsilon'')^2} \tag{4}$$

The real modulus (M') and imaginary modulus (M'') of according to the relaxation of the electric field are given an indication of electrical properties. Using the complex modulus data, the values of M' and M'' were calculated as [37]:

$$M' = \frac{\varepsilon'}{(\varepsilon'^2 + \varepsilon'''^2)} \tag{5}$$

$$M'' = \frac{\varepsilon''}{(\varepsilon'^2 + \varepsilon'''^2)} \tag{6}$$

Fig. 11 shows the relation between the real part (M) for electrical modulus with frequency Log (f) at room temperature. The behavior of M' is observed increase with the increase of

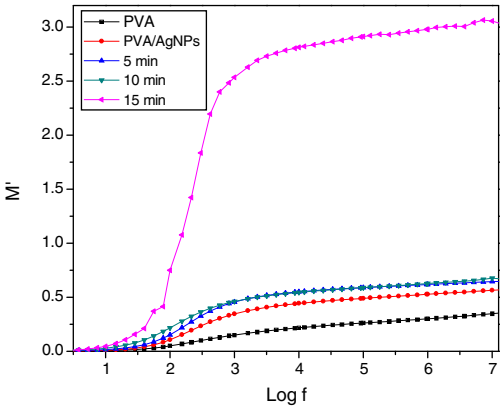

Fig. 11 – Dependence of real electrical modulus (M′) with frequency for pure PVA and PVA/Ag nanocomposite films before and after irradiated to different times of nanosecond laser (5, 10, 15 min) at room temperature.

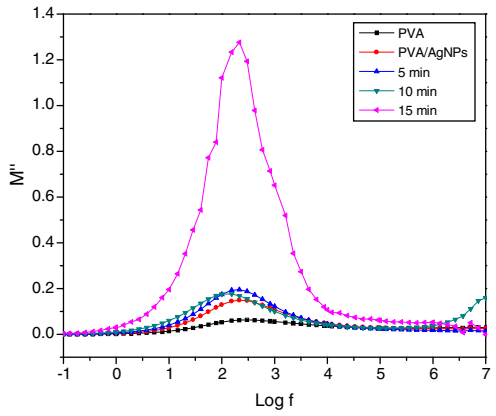

Fig. 12 – Dependence of imaginary electrical modulus (M″) with frequency for pure PVA and PVA/Ag nanocomposite films before and after irradiated to different times of nanosecond laser (5, 10, 15 min) at room temperature.

frequency an AgNPs cause an increase of the ionic conduction of the samples. Fig. 12 shows the graph between the imaginary part (M″) and Log (f) at room temperature. The broad peak of M″ is observed and it increases with the increase of frequency indicating an indication to the nature of the relaxation processes exist. The presence of peack in electrical modulus confirm that samples are ionic conductors. The increase of M″ peack with increase of AgNPs and shifted toward the higher frequencies are clear. Also, the maximum value of the M″ peak increases for the doped samples compared to the pure blend suggesting that the AgNPs contributes to the relaxation process.

3.4.3. *Modulus study*

The study of the electrical modulus is utilized for better understanding of the dielectric relations of the prepared samples and can be used to explore the relaxation of conductivity by suppressing the polarization effect at low frequency. Thus, the dielectric information is changed into the modulus information and can be identified with the permittivity from Eqs. (5) and (6). Fig. 13 displays the plot of real part (M) virus imaginary part (M″) for the samples. The plot for all spectra shows the formation of a semicircle arc indicating the presence of broad relaxation processes [38]. The existence of a single semicircle is the significance of single relaxation inside the nanocomposites. The little of radius semi-circle is related with the highest capacitance.

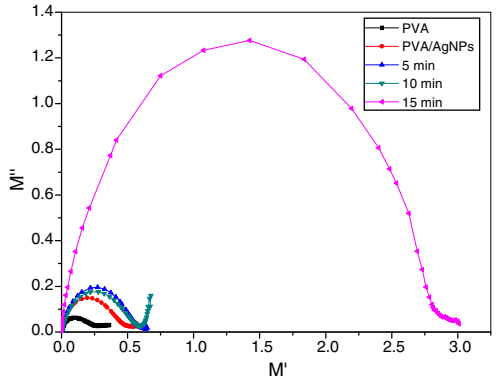

Fig. 13 – Debye-type complex electric modulus plane plots (M″ vs M′) for pure PVA and PVA/Ag nanocomposite films before and after irradiated to different times of nanosecond laser (5, 10, 15 min) at room temperature.

4. Conclusion

The nanocomposite films of PVA/Ag were synthesized via chemical reduction technique. PVA/AgNPs films were irradiated to different times (5, 10, 15 min) pulsed Nd:YAG nanosecond laser. According to the discussion, it was observed that influences of the different laser irradiation times on the films make a sufficient change in the structural, optical, and electrical properties of PVA/Ag nanocomposites. The integral intensity of diffracted X-ray photons from films has been increased noticeably after the doping process indicate the increase in the ordering character of the PVA/Ag nanocomposites irradiated to different time's laser, which can be assigned to the reduction that has been induced by laser. Observations of IR spectra indicated that laser enhances the structural modifications between the silver nanoparticles and the chains in PVA with further increasing laser irradiation time. The observed increase in refractive index (*n*) and, the decreasing in the optical energy band gap of PVA/Ag nanocomposites films after irradiated to the laser with different times comparing with pure PVA suggesting its possibility to using optical device applications. The plots of both ε' and ε'' are gradually decrease with the increase of the frequency and it reaches to constant values at higher frequency. At low frequencies, the values of ε' and ε'' are decreases due to the contribution of interfacial polarization effect in dielectric permittivity. The increase of M″ peak with increase of AgNPs and shifted toward the higher frequencies are clear. The plot M′ versus imaginary part M″ shows the formation of semicircle arc indicating the presence of broad relaxation processes.

Conflicts of interest

The authors declare no conflicts of interest.

REFERENCES

[1] Monika T, Dhruv T. Polymer nanocomposites and their applications in electronics industry. Int J Electron Electr Eng 2014;7:603–8.
[2] Adelung R, Aktas OC, Franc J, Biswas A, Kunz R, Elbahri M, et al. Strain-controlled growth of nanowires within thin-film cracks. Nat Mater 2004;3(6):375–9.
[3] Hopkins DS, Pekker D, Goldbart PM, Bezryadin A. Quantum interference device made by DNA templating of superconducting nanowires. Scinece 2005;308(5729):1762–5.
[4] Ananth AN, Umapathy S. On the optical and thermal properties of in situ/ex situ reduced Ag NP's/PVA composites and its role as a simple SPR-based protein sensor. Appl Nanosci 2011;1(2):87–96.
[5] Abd El-kader FH, Hakeem NA, Elashmawi IS, Menazea AA. Synthesis and characterization of PVK/AgNPs

nanocomposites prepared by laser ablation. Spectrochem Acta A 2015;138:331–9.
[6] Dawy M, Rifaat HM, Menazea AA. Characterization of Ag nanoparticles by nanosecond pulsed laser ablation doped in chitosan. Curr Sci Int 2015;4:621–7.
[7] Menazea AA, Elashmawi IS, Abd El-kader FH, Hakeem NA. Nanosecond pulsed laser ablation in liquids as new route for preparing polyvinyl carbazole/silver nanoparticles composite: spectroscopic and thermal studies. J Inorg Organomet Polym Mater 2018;28:2564–71.
[8] Twu YK, Chen YW, Shih CM. Preparation of silver nanoparticles using chitosan suspensions. Powder Technol 2008;185:251–7.
[9] Ray S, Easteal AJ, Cooney RP, Edmonds NR. Structure and properties of melt-processed PVDF/PMMA/polyaniline blends. Mater Chem Phys 2009;113:829–38.
[10] Habisreutinger SN, Leijtens T, Eperon GE, Stranks SD, Nicholas RJ, Snaith HJ. Carbon nanotube/polymer composites as a highly stable hole collection layer in perovskite solar cells. Nano Lett 2014;14(10):5561–8.
[11] Weickmann H, Tiller JC, Thomann R, Mulhaupt R. Metallized organoclays as new intermediates for aqueous nanohybrid dispersions, nanohybrid catalysts and antimicrobial polymer hybrid nanocomposites. Macromol Mater Eng 2005;290(9):875–83.
[12] Peponi L, Puglia D, Torre L, Valentini L, Kenny JM. Processing of nanostructured polymers and advanced polymeric based nanocomposites. Mater Sci Eng: R: Rep 2014;85:1–46.
[13] Dhibar S, Das CK. Silver nanoparticles decorated polyaniline/multiwalled carbon nanotubes nanocomposite for high-performance supercapacitor electrode. Ind Eng Chem Res 2014;53(9):3495–508.
[14] Clemenson S, Leonard D, Sage D, David L, Espuche E. Metal nanocomposite films prepared in situ from PVA and silver nitrate. Study of the nanostructuration process and morphology as a function of the in situ routes. J Polym Sci 2008;46(6):2062–71.
[15] Fussell G, Thomas J, Scanlon J, Lowman A, Marcolongo M. The effect of protein-free versus protein-containing medium on the mechanical properties and uptake of ions of PVA/PVP hydrogels. J Biomater Sci Polym 2005;16(4):489–503.
[16] Abargues R, Marqués-Hueso J, Canet-Ferrer J, Pedrueza E, Valdés JL, Jiménez E, et al. High-resolution electron-beam patternable nanocomposite containing metal nanoparticles for plasmonics. J Nanotechnol 2008;19(35):355308–14.
[17] Abargues R, Gradess R, Canet-Ferrer J, Abderrafi K, Valdes JL, Martinez-Pastor J. Scalable heterogeneous synthesis of metallic nanoparticles and aggregates with polyvinyl alcohol. J New Chem 2009;33:913–7.
[18] Morsi MA, RajehA, Menazea AA. Nanosecond laser-irradiation assisted the improvement of structural, optical and thermal properties of polyvinyl pyrrolidone/carboxymethyl cellulose blend filled with gold nanoparticles. J Mater Sci: Mater Electron 2018, http://dx.doi.org/10.1007/s10854-018-0545-4.
[19] Gautam A, Ram S. Preparation and thermomechanical properties of Ag-PVA nanocomposite films. Mater Chem Phys 2010;119:266–71.
[20] Nouh SA, Benthami K, Alhazime AA, Almarashi JQ. Structural, thermal and optical behavior of laser irradiation-induced PVA–PEG–Ag nanocomposites. Radiat Eff Defects Solids 2017;172(3–4):275–85.
[21] Nouh SA, Nagla AG, Othman MH, Eman SA, Lotfi ZI. Thermal, structural, and optical properties of γ irradiated poly (vinyl alcohol)/poly(ethylene glycol) thin film. J Appl Polym Sci 2012;124:654–60.
[22] Elashmawi IS, Abdelrazek EM, Hezma AM, Rajeh A. Modification and development of electrical and magnetic properties of PVA/PEO incorporated with $MnCl_2$. Phys B: Condens Matter 2014;434:57–63.
[23] Suo B, Su X, Wu J, Chen D, Wang A, Guo Z. Poly (vinyl alcohol) thin film filled with CdSe-ZnS quantum dots: fabrication, characterization and optical properties. Mater Chem Phys 2010;119(1–2):237–42.
[24] Meng Y. A sustainable approach to fabricating Ag nanoparticles/PVA hybrid nanofiber and its catalytic activity. Nanomaterials 2015;5(2):1124–35.
[25] Abd El-Kader KAM, Abdel Hamied SF. Preparation of poly(vinyl alcohol) films with promising physical properties in comparison with commercial polyethylene film. J Appl Polym Sci 2002;86:1219–26.
[26] Chahal RP, Mahendia S, Tomar AK, Kumar S. γ Irradiated PVA/Ag nanocomposite films: materials for optical applications. J Alloys Compd 2012;538:212–9.
[27] Omer MA, Ismail HA, Garlnabi ME, Edam GA, Mustafa NS. Optimization of PAV\$AgNO_3$ films for measuring entrance and exit radiotherapy dose relative to TLDs. Int J Sci Res 2015;4:1279–82.
[28] Baraz N, Yucedag I, Kalandaragh YA, Altındal S. Determining electrical and dielectric parameters of dependence as function of frequencies in Al/ZnS-PVA/p-Si (MPS) structures. J Mater Sci: Mater Electron 2017;28(2):1315–21.
[29] Harun MH, Saion E, Kassim A, Mahmud E, Hussain MY, Mustafa IS. Dielectric properties of poly (vinyl alcohol)/polypyrrole composite polymer films. J Adv Sci Arts 2009;1(1):9–16.
[30] Ananth AN, Umapathy S, Sophia J, Mathavan T, Mangalaraj D. On the optical and thermal properties of in situ/ex situ reduced Ag NP's/PVA composites and its role as a simple SPR-based protein sensor. Appl Nanosci 2011;1(2):87–96.
[31] Ghanipour M, Dorranian D. Effect of Ag-nanoparticles doped in polyvinyl alcohol on the structural and optical properties of PVA films. J Nanomater 2013, http://dx.doi.org/10.1155/2013/897043.
[32] Dimitrov V, Sakka S. Linear and nonlinear optical properties of simple oxides. II. J Appl Phys 1996;79(3):1741–5.
[33] Mohamed SA, Al-Ghamdi AA, Sharma GD, El Mansy MK. Effect of ethylene carbonate as a plasticizer on CuI/PVA nanocomposite: structure, optical and electrical properties. J Adv Res 2014;5(1):79–86.
[34] Rajeh A, Morsi M, Elashmawi IS. Enhancement of spectroscopic, thermal, electrical and morphological properties of polyethylene oxide/carboxymethyl cellulose blends: combined FT-IR/DFT. Vacuum 2019;159:430–40.
[35] Polu AR, Kumar R. AC impedance and dielectric spectroscopic studies of Mg^{2+} ion conducting PVA–PEG blended polymer electrolytes. Bull Mater Sci 2011;34(5):1063–7.
[36] Langar A, Sdiri N, Elhouichet H, Ferid M. Structure and electrical characterization of ZnO-Ag phosphate glasses. Res Phys 2017;7:1022–9.
[37] Tripathi SK, Gupta A, Kumari M. Studies on electrical conductivity and dielectric behaviour of PVdF–HFP–PMMA–NaI polymer blend electrolyte. Bull Mater Sci 2012;35(6):969–75.
[38] Mahapatra T, Halder S, BhuyanS, Choudhary RNP. Dielectric and electrical characterization of lead-free complex electronic ceramic: $(Bi_{1/2}Li_{1/2})(Zn_{1/2}W_{1/2})O_3$. J Mater Sci Mater Electron 2014;29(21):18742–50.